

## Marine snow, organic solute plumes, and optimal chemosensory behavior of bacteria

Thomas Kiørboe

Danish Institute for Fisheries Research, Kavalergaarden 6, DK-2920 Charlottenlund, Denmark<sup>1</sup>

George A. Jackson

Department of Oceanography, Texas A&M University, College Station, Texas 77843

### Abstract

Leaking organic solutes form an elongated plume in the wake of a sinking aggregate. These solutes may both be assimilated by suspended bacteria and guide bacteria with chemokinetic swimming behavior toward the aggregate. We used modifications of previously published models of the flow and concentration fields around sinking aggregates and of chemokinetic behavior of bacteria to identify the behavior that optimizes aggregate colonization and plume utilization. The optimal solution is governed by physical constraints and is a trade off between a high sensitivity to chemical signals and a long signal integration time. For a run-and-tumble swimming behavior, the predicted tumbling frequency is between 1 and 10 s<sup>-1</sup>, similar to that reported for marine bacteria. The predicted optimal sensitivity to chemical signals is similar to or greater than that known for *Escherichia coli*. The optimal behavior was used to examine the potential contribution of aggregate-generated solute plumes for water column bacterial production. Despite occupying only a small volume fraction, the plumes may provide important growth habitats for free bacteria and account for a significant proportion of water column bacterial production at typical concentrations of marine snow aggregates.

Many marine bacteria have well-developed chemokinetic swimming behaviors. They modify their motilities in response to gradients in the concentration of certain molecules. This type of behavior results in a net movement toward or away from sources of attractor and repellent molecules, respectively, or toward regions with optimal concentrations of certain molecules (e.g., oxygen). There are numerous observations of this type of behavior in marine bacteria (Fenchel 1994; Mitchell et al. 1996; Blackburn et al. 1998). Thus, bacteria—including pelagic ones—appear to be adapted to navigate in a heterogeneous environment.

The pelagic environment is, in fact, heterogeneous, also with respect to the small-scale distribution of organic solutes. Ephemeral point sources of dissolved organic matter (DOM) arise whenever protists or other small organisms lyse. Bacteria are attracted to these sources (Blackburn et al. 1998). Likewise, larger zooplankton feeding on smaller particles may cause localized spillage of DOM (Lampert 1978), and zooplankton fecal pellets can leak DOM at high rates (Urban-Rich 1999), generating short-lived patches of DOM. Additional and potentially significant sources of DOM plumes are the large aggregates known as marine snow. Bacteria residing on aggregates appear to solubilize particulate material faster than they absorb the resulting solutes (Vetter et al. 1998), leading to high concentrations of DOM in the interior of aggregates (Alldredge 2000) and substantial leakage of DOM from sinking aggregates (Smith et al. 1992; Grossart and Simon 1998). The combined effect of diffusion

and advection results in an elongated solute plume trailing behind the sinking aggregate (Kiørboe et al. 2001; Fig. 1). The volume of the plume holding DOM concentrations high enough to impact bacterial growth may be 1–2 orders of magnitude larger than the volume of the aggregate itself. Even though the combined volume of plumes from all occurring aggregates may occupy only a relatively small fraction of the water volume, the plumes may have a disproportionate effect on bacterial growth dynamics because bacteria in the vicinity of a sinking aggregate may experience long retention times in the plume by being entrained in the boundary layer. In addition, bacteria with chemokinetic behavior may actively increase their residence times inside the plume and benefit from the elevated solute concentration in the wake of a sinking aggregate. Because marine snow aggregates occur in all aquatic environments, sometimes at high concentrations (Alldredge and Silver 1988), DOM leaking from aggregates may provide a significant and reactive source of DOM in the pelagic environment, and the plumes with elevated concentration of DOM may be sites of significant bacterial growth.

The purpose of the present work was to examine the contribution of aggregate solute plumes to population level bacterial growth and production in the pelagic environment. We used modifications of previously published models of the flow and concentration field around a sinking aggregate (Kiørboe et al. 2001) and of the chemokinetic swimming behavior of bacteria (Brown and Berg 1974; Jackson 1987, 1989; Bowen et al. 1993) to determine the optimal bacterial behavior for aggregate colonization and plume utilization. We next examined how aggregate colonization and plume utilization scale with aggregate size. Finally, we combined the findings with observed aggregate size spectra to assess the integrated effect on the growth of free bacteria in the pelagic environment.

<sup>1</sup> Corresponding author (TK@DFU.MIN.DK).

### Acknowledgments

We benefited from advice on modeling issues from Uffe H. Thygesen. This research was supported by grants from the Danish Natural Science Research Council (9801393) to T.K. and the United States National Science Foundation (OCE-9726077) to G.J.

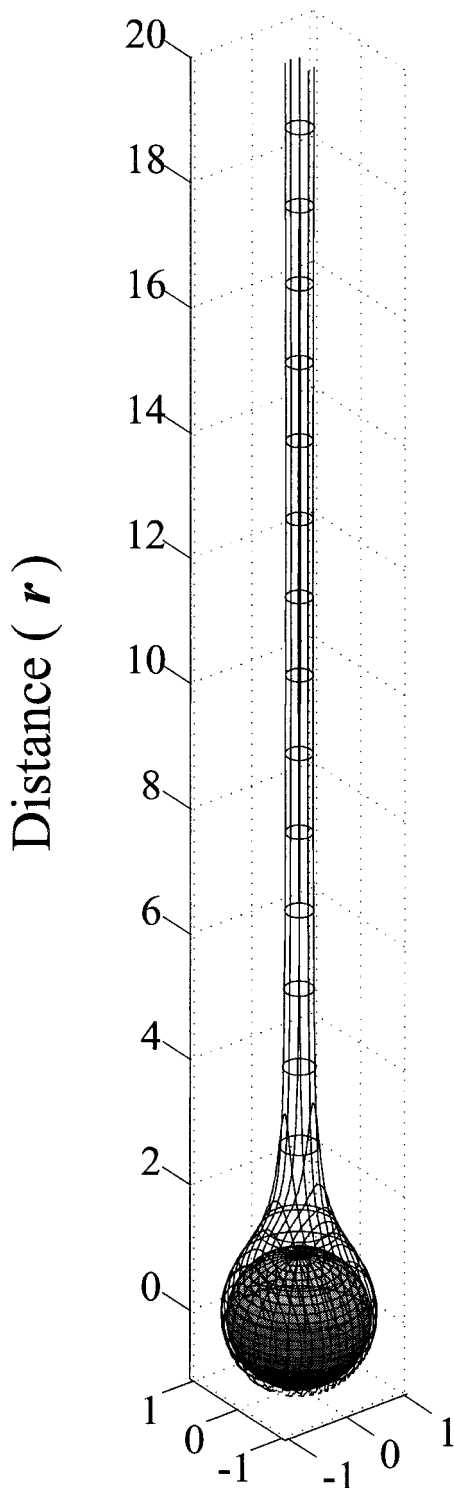


Fig. 1. Graphic showing the plume streaming behind a falling aggregate 0.5 cm in radius. Distances are in units of aggregate radius. The plume border corresponds to an amino acid concentration  $3 \times 10^{-11} \text{ mol cm}^{-3}$  above ambient concentration. Figure taken from Kiørboe et al. (2001).

## The model

*Fluid flow and solute distribution around sinking aggregate*—We have previously modeled the flow and concentration fields around a sinking, impermeable spherical aggregate (Kiørboe et al. 2001; Thygesen and Kiørboe unpubl. data). The scaled flow field can be characterized solely by the Reynolds number ( $Re = rU/\nu$ ), where  $r$  is aggregate radius,  $U$  is aggregate sinking velocity, and  $\nu$  is kinematic viscosity ( $10^{-2} \text{ cm}^2 \text{ s}^{-1}$ ) (see Table 1 for definition of symbols). The flow is described by solving the Navier-Stokes equations numerically. The concentration field is determined by subsequently solving the advection-diffusion equation. The concentration field can then be characterized by the Peclet number ( $Pe = rU/D$ ) and the leakage rate of solutes,  $Q_r$ , where  $D$  is the diffusion coefficient of the solute ( $\sim 10^{-5} \text{ cm}^2 \text{ s}^{-1}$ ). We assumed that solute flow was reaction rather than transport limited (i.e., applying a Neumann boundary condition; see Kiørboe et al. 2001) and used amino acids and nitrogen as the currency of organic solutes (1 mol N  $\sim$  1 mol amino acid). Computations we made for aggregates varying in size between  $\sim 0.02$  and 1.5 cm radius. We applied empirically derived relations for aggregate sinking velocity ( $U_r$ ) and amino acid leakage rate ( $Q_r$ ) as a function of aggregate size in our calculations:

$$U_r \text{ (cm s}^{-1}\text{)} = 0.13r_{cm}^{0.26} \quad \text{(Alldredge and Ghotschalk 1988),} \quad (1)$$

$$Q_r \text{ (mol s}^{-1}\text{)} = 10^{-12}r_{cm}^{1.5} \quad \text{(Kiørboe et al. 2001).} \quad (2)$$

The solute plume trailing behind the sinking aggregate was defined as the region holding amino acid concentrations exceeding  $3 \times 10^{-11} \text{ mol cm}^{-3}$ , a value chosen to represent the region with a concentration greater than the typical half-saturation concentration for amino acid uptake in marine bacteria (see Kiørboe et al. 2001). Background concentration was assumed to be zero.

*Bacterial chemosensory behavior*—We used the model of Brown and Berg (1974) as implemented by Jackson (1987, 1989) to describe the chemokinetic behavior of the bacteria. It is assumed that the bacteria swim in straight runs interrupted by occasional tumbles, when the bacterium changes swimming direction randomly. When the bacterium experiences increasing amino acid concentration during a run, the probability of tumbling decreases and vice versa during runs with decreasing concentration. This behavior leads to positive chemokinesis. The probability of tumbling within the time interval  $\Delta t$  is (Jackson 1989)

$$P_t = \Delta t/\tau, \quad (3)$$

where  $\tau$  is the mean run time, given by

$$\ln \tau = \ln \tau_0 + \alpha \frac{\overline{dP_b}}{dt}, \quad (4)$$

Table 1. Symbols used, default parameter values.

Sym- bol	Description	Units	Default value
$C$	Amino acid concentration	$\text{mol cm}^{-3}$	
$D_r$	Bacterial rotational diffusivity	$\text{rad}^2\text{s}^{-1}$	0.5
$D$	Diffusion coefficient	$\text{cm}^2\text{s}^{-1}$	$10^{-5}$
$K_D$	Half saturation constant for chemokinetic responsiveness	$\text{mol cm}^{-3}$	—
$Q_r$	Amino acid leakage rate	$\text{mol s}^{-1}$	$10^{-12} r_{\text{cm}}^{1.5}$
$r$	Aggregate radius	cm	0.02–1.5
$T_m$	Bacterial time constant	s	—
$U$	Aggregate sinking velocity	$\text{cm s}^{-1}$	$0.13 r_{\text{cm}}^{0.26}$
$v_0$	Bacterial swimming velocity	$\text{cm s}^{-1}$	$0.01 \text{ cm s}^{-1}$
$\alpha$	System time constant	s	660
$\Delta t$	Computational time step	s	0.01
$\kappa$	Bacterial capture clearance rate	$\text{cm}^3 \text{s}^{-1}$	—
$\beta$	Bacterial uptake clearance rate	fractional uptake $\times \text{cm}^3\text{s}^{-1}$	—
$\nu$	Kinematic viscosity	$\text{cm}^2\text{s}^{-1}$	—
$\tau$	Mean run time in the presence of concentration gradients	s	—
$\tau_0$	Mean run time in absence of concentration gradient	s	—
$\mu$	Bacterial specific growth rate	$\text{s}^{-1}$	—

$$\overline{\frac{dP_b}{dt}} = T_m^{-1} \int_{-\infty}^t \frac{dP_b}{dt'} \exp\left[\frac{(t' - t)}{T_m}\right] dt', \quad (5)$$

$$\frac{dP_b}{dt} = \frac{K_D}{(K_D + C)^2} \frac{dC}{dt}, \quad (6)$$

where  $T_m$  is a time constant of the bacterial system (a memory term),  $\tau_0$  is the mean run time (tumbling interval) in the absence of concentration gradients,  $C$  is amino acid concentration,  $\alpha$  is a system time constant (amplification factor),  $P_b$  is the fraction of surface receptors bound by the substrate,  $(dP_b/dt)$  is a weighted rate of change of  $P_b$ , and  $K_D$  is the half-saturation constant of the surface receptor binding to amino acids. Default values of the constants used in the simulations are listed in Table 1. We considered two bacterial swimming speeds, 10 and 100  $\mu\text{m s}^{-1}$ . The former is similar to that used in previous simulations (Jackson 1987, 1989), and the latter is more representative of swimming speeds of marine bacteria (Fenchel 1994; Mitchell et al. 1995*a,b*; Barbara and Mitchell 1996; Mitchell and Barbara 1999). For the amplification factor,  $\alpha$ , we assumed a value similar to that estimated for *Escherichia coli*, 660 s (Brown and Berg 1974), and  $K_D$  and  $\tau_0$  were estimated as described below.

The swimming tracks between tumbles are in reality not really straight, because Brownian rotation will slightly and continuously change the swimming direction. We included the effect of Brownian rotation as in Jackson (1987) by assuming a rotational diffusivity of  $0.5 \text{ rad}^2 \text{ s}^{-1}$ .

We included the effect of fluid deformation and vorticity on bacterial swimming direction and on colonization rates. Because most motile bacteria are elongated (Dusenbery 1998), they will tend to align in a sheared flow field such as the one that occurs along the sides of the aggregate. We computed the deformation and vorticity fields according to the methods in Kiørboe and Visser (1999) and used the for-

mulations of Visser and Jonson (1999) to calculate the (re)orientation of the bacteria at each time step. Because swimming bacteria are elongated with an aspect ratio of on average 3 (Dusenbery 1998) and are equipped with a long rigid flagellum, we assumed a shape-factor of 1 in the computations (see Visser and Jonson 1999). We also examined the effect of a back-and-forth swimming behavior instead of the run-tumble behavior, because the former is characteristic for some marine bacteria (Blackburn et al. 1998; Luchsinger et al. 2000).

*Optimal chemokinetic behavior for aggregate colonization and plume utilization*—The parameters in the chemokinetic behavioral model have been estimated for *E. coli* but are not known for marine bacteria. For example,  $K_D$ , the half saturation constant for chemosensing, has been estimated for *E. coli* to be  $\sim 10^{-7} \text{ mol cm}^{-3}$  for  $\alpha$ -methylaspartate (Mesibov et al. 1973), a value that has been used in previous models (e.g. Jackson 1987, 1989; Blackburn et al. 1998). However, one could imagine that marine bacteria that survive in a nutritionally more dilute environment than enteric bacteria may have developed a higher sensitivity. There are, however, kinetic constraints on the magnitude of  $K_D$ , because higher sensitivities (lower  $K_D$ ) require longer integration times (essentially longer tumbling intervals). If the time interval between tumbles is too long, then a bacterium could pass by a region of high concentration before it responds. There is, therefore, a trade off between long tumbling intervals and high sensitivity. We sought the combination of the two that yields the highest aggregate or plume colonization rates.

In quantitative terms, the half-saturation constant can be described as the ratio between the constants describing the rate at which attractor molecules react (bind) with the cell surface receptors ( $k_1$ ), and the constant describing the regeneration rate of unbound receptors ( $k_2$ ):

$$K_D = k_2/k_1 \quad \text{or} \quad k_2 = K_D k_1. \quad (7)$$

The disassociation constant,  $k_2$ , represents the rate at which the system “forgets” its past and corresponds most closely to  $T_m^{-1}$  in the Brown and Berg model. It is also related to the mean run time,  $\tau_0$ , because  $\tau_0 \geq T_m$  (Jackson 1987). Equation 7 places bounds on  $k_2$ . The rate of reaction between 2 molecules ( $k_1$ ) is constrained by diffusion. If we use the extremely rapid rate for EDTA-iron,  $k_1 = 10^9 \text{ cm}^3 \text{ s}^{-1} \text{ mol}^{-1}$  (Jackson and Morgan 1978), then we will have an effective upper bound on  $k_2$  and, hence, a lower bound on  $T_m$  and  $\tau_0$ , for a given value of  $K_D$ . A greater sensitivity to low concentrations (small  $K_D$ ) results in a lower sensitivity to short pulses (smaller  $k_2$ ) and hence requires a longer integration time and a longer tumbling interval. On the basis of these considerations, we assumed

$$\tau_0 \geq T_m \text{ (s)} = 10^{-9} \text{ (mol s cm}^{-3}\text{)}/K_D \text{ (mol cm}^{-3}\text{)}. \quad (8)$$

**Simulations**—In a typical simulation, we started 10,000 bacteria in a horizontal row 10 aggregate radii below the aggregate out to a horizontal distance from the fall line of 1 or 4 radii for slow- and fast-swimming bacteria, respectively. The bacteria were distributed such that their distribution represented a uniform distribution in the plane. The simulations were run until most or all the bacteria had left the plume again behind the aggregate. We kept track of the position and ambient amino acid concentration experienced by individual bacteria at each time step ( $\Delta t = 0.01 \text{ s}$ ). This allowed us to compute various properties, such as the fraction of bacteria inside the plume at any time, the number of bacteria hitting (colonizing) the aggregate, etc., that were used to evaluate the effect of various behaviors. The assumed initial distribution of bacteria ignores the effect of bacteria diffusing in from the sides. However, this effect is small as long as the bacterial Peclet number,  $Pe_{\text{bact}}$ , is much larger than 1 (in our standard simulations  $Pe_{\text{bact}} = Ur/D_{\text{bact}} > 33$ , where  $D_{\text{bact}} = \tau\nu_0^2/6$ ).

To identify the chemokinetic behavior that leads to either the highest aggregate colonization rate or to optimal utilization of the plume, we varied bacterial swimming characteristics ( $\tau_0$ ) and chemosensory characteristics ( $K_D, T_m$ ) within the constraints given by Eq. 8. Colonization rate was expressed as a capture clearance rate (the imaginary volume of water “cleared” for bacteria by the sinking aggregate per unit time), whereas plume utilization was quantified as the average enhancement of bacterial concentration inside the plume due to chemokinetic behavior (ratio of average concentration with and without chemokinetic behavior; the latter estimated by putting  $K_D = 10^8 \text{ mol cm}^{-3}$ ). We first performed simulations where  $K_D$  was varied between  $10^{-7}$  and  $10^{-11} \text{ mol cm}^{-3}$  with  $T_m = \tau_0$ ; this corresponds to  $T_m$  and  $\tau_0$  varying between 0.01 and 100 s. Because the constraint in  $\tau_0$  is that it has to be larger than  $T_m$ , we next fixed  $K_D (= 10^{-8} \text{ mol cm}^{-3})$  and  $T_m (= 0.1 \text{ s})$  and varied  $\tau_0$  between 0.1 and 10 s to examine the effect of  $\tau_0$ . All simulations were done for a small ( $r = 0.021 \text{ cm}$ ,  $Re = 1$ ) and a large ( $r = 0.81 \text{ cm}$ ,  $Re = 10$ ) aggregate.

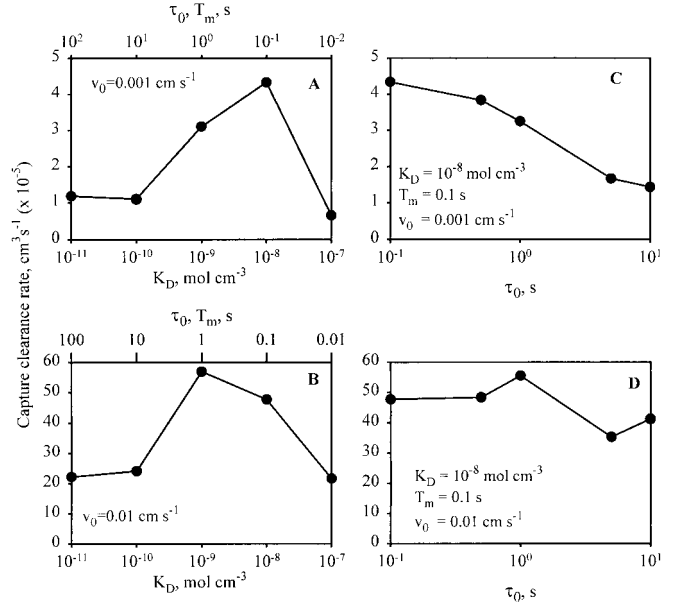


Fig. 2. Effect of variable bacterial constants on aggregate colonization for  $Re = 1$ , corresponding to a 0.021-cm-radius aggregate. (A) and (B),  $K_D$  has been varied between  $10^{-7}$  and  $10^{-11} \text{ mol cm}^{-3}$  and  $T_m = \tau_0$  between  $10^{-2}$  and  $10^2 \text{ s}$ . (C) and (D),  $K_D$  and  $T_m$  are fixed (at  $10^{-8} \text{ mol cm}^{-3}$  and 0.1 s, respectively), whereas  $\tau_0$  has been varied between 0.1 and 10 s. Bacterial swimming velocity,  $v_0$ , is either  $0.001 \text{ cm s}^{-1}$  (A and C) or  $0.01 \text{ cm s}^{-1}$  (B and D).

## Results and discussion

**Optimal behavior**—Aggregate colonization: The collision rate between bacteria and an aggregate depends both on the motility of the bacteria (swimming speed and tumbling frequency) and on the chemosensory response of the bacteria. It is the total effect that counts. There is an optimum in the net relationship among  $K_D$ ,  $T_m$ , and  $\tau_0$  on the one hand and colonization rate (capture clearance rate) on the other (Figs. 2A,B, 3A,B). With fixed values of  $T_m$  and  $K_D$ , the clearance rate decreases slightly with increasing length of the tumbling interval (Figs 2C,D, 3C,D). Thus, the smallest possible tumbling interval with the optimal sensitivity yields the highest colonization rate. The position of the optimum varies as a function of aggregate sinking velocity and bacterial swimming velocity. With both velocities increasing, the optimum changes toward greater sensitivity (smaller  $K_D$ ) and longer tumbling interval. The optimum varies between  $K_D = 10^{-8}$  and  $10^{-9} \text{ mol cm}^{-3}$  and  $\tau_0$  between 0.1 and 1 s.

**Plume utilization:** For the slowly swimming bacteria, plume utilization is independent of swimming and chemosensory characteristics for both small and large aggregates (Figs. 4, 5), because the slowly swimming bacteria are unable to enhance their residence times in the plume. In other words, a chemokinetic response does not allow the slowly swimming bacteria to utilize the enhanced concentration of solutes in the downstream plume better than bacteria without a chemokinetic response. Faster swimming bacteria, in contrast, are able to optimize their plume utilization for some values of  $K_D$ ,  $T_m$ , and  $\tau_0$ . The optimum again occurs with the shortest possible run length (Figs. 4, 5). The optimal en-

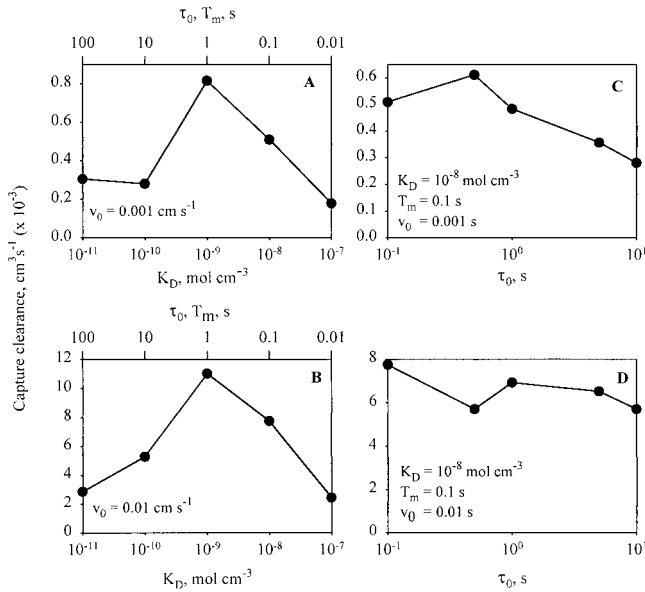


Fig. 3. Effect of variable bacterial constants on aggregate colonization for  $Re = 10$ , corresponding to a 0.81-cm-radius aggregate. Values of parameters as for Fig. 2.

hancement in bacterial concentration inside the plume is modest, a factor of 2–3. For plume utilization, the optimum is again close to  $K_D = 10^{-9}$  mol  $cm^{-3}$  and  $\tau_0 \sim 1$  s.

Effect of swimming mode and shear alignment: Changing the assumed bacterial swimming mode from run-and-tumble to back-and-forth does not change either colonization rate or plume utilization noticeably (Fig. 6A,B). Likewise, shear alignment has little effect on the efficiency with which bacteria colonize the aggregate and stay in the downstream plume. Therefore, in all subsequent computations we assume

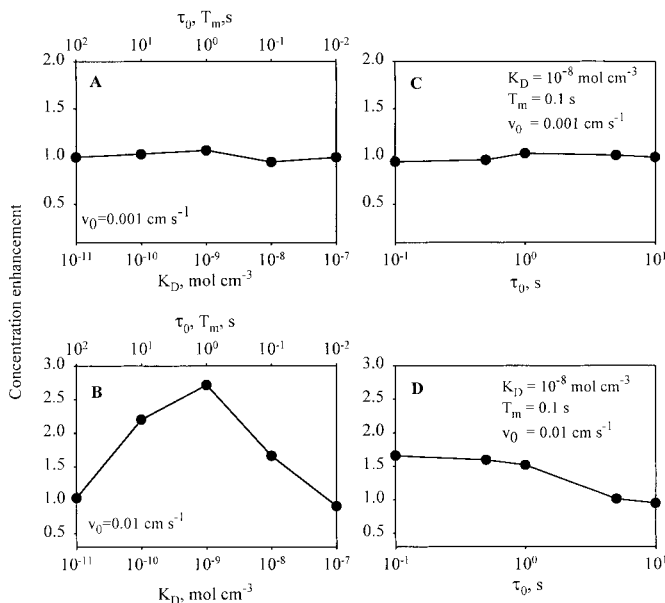


Fig. 4. Effect of variable bacterial constants on plume utilization for  $Re = 1$  ( $r = 0.021$  cm). Values of parameters as for Fig. 2.

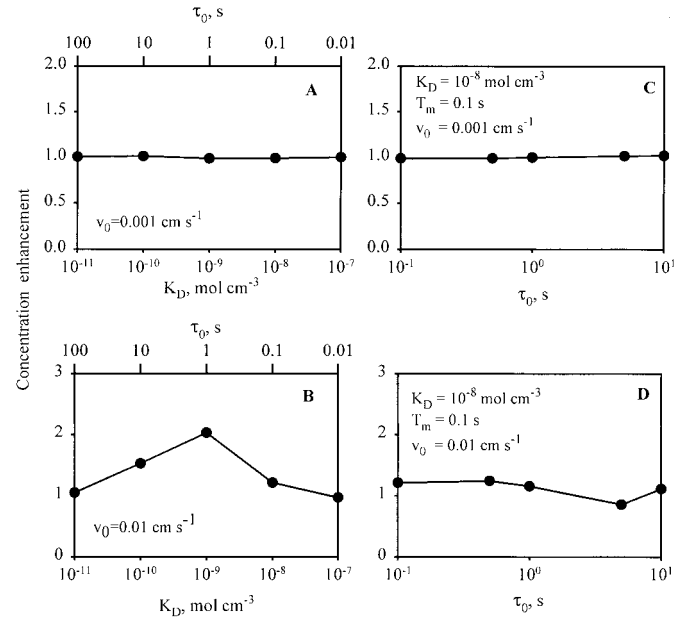


Fig. 5. Effect of variable bacterial constants on plume utilization for  $Re = 10$  ( $r = 0.81$  cm). Values of parameters as for Fig. 2.

a run-and-tumble swimming mode and ignore the effect of shear alignment.

Optimal behavior: The optimal combination of chemical sensitivity ( $K_D$ ) and bacterial integration time ( $T_m$ ,  $\tau_0$ ) is similar for aggregate colonization and plume utilization. The predicted optimal tumbling interval, 0.1–1 s, is very similar to the tumbling interval reported for marine bacteria (Mitch-

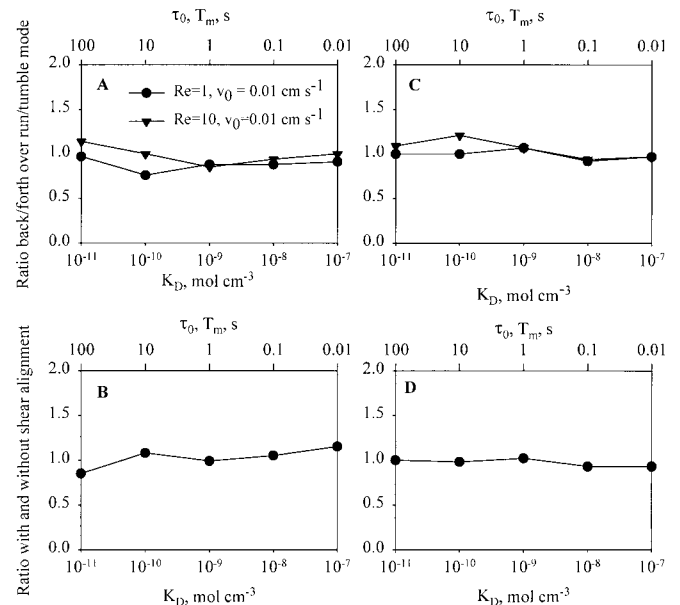


Fig. 6. Effect of bacterial swimming mode on (A) aggregate colonization and (C) plume utilization and effect of shear alignment on (B) aggregate colonization and (D) plume utilization. Parameter values as for Fig. 2, except that bacterial swimming velocity is 0.01  $cm\ s^{-1}$  in all plots.

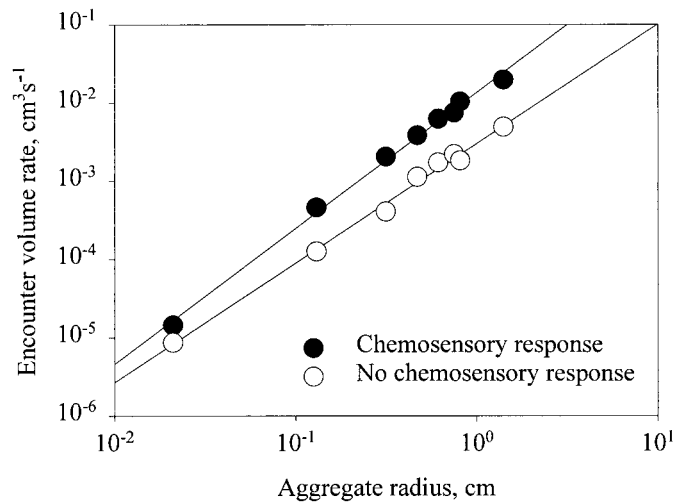


Fig. 7. Bacterial colonization of aggregates ( $\kappa$ ,  $\text{cm}^3 \text{s}^{-1}$ ) as a function of aggregate radius ( $r$ , cm) and chemosensory behavior. The regression lines are: without chemosensory response,  $\log \kappa = -2.51 + 1.53 \log r$ , and with chemosensory response,  $\log \kappa = -1.86 + 1.74 \log r$ . Computations are based on bacterial swimming velocity  $v_0 = 100 \mu\text{m s}^{-1}$  and  $\tau_0 = 1$  s. For chemosensory bacteria,  $K_D = 10^{-9} \text{mol cm}^{-3}$ .

ell et al. 1996; Blackburn et al. 1998). There are no estimates available for values of  $K_D$  for marine bacteria, and the optimum predicted here is substantially less than that found for *E. coli* detecting amino acids. Our estimate is probably a minimum estimate (i.e., maximum sensitivity) because we used a particularly high value of  $k_1$  to constrain  $K_D$ . However, values of this magnitude ( $10^{-9} \text{mol cm}^{-3}$ ) have been reported for *E. coli* for D-galactose (Mesibov et al. 1973). In all subsequent calculations, we use  $K_D = 10^{-9} \text{mol cm}^{-3}$  for the bacteria with chemokinetic behavior. For bacteria without chemokinetic behavior, we just put  $K_D$  very high ( $10^8 \text{mol cm}^{-3}$ ). For both, we assume  $\tau_0 = 1$  s and  $v_0 = 0.01 \text{cm s}^{-1}$ .

**Scaling of colonization rate**—The dynamics of marine snow microbial communities depend on both the (local) growth and mortality rates as well as on the colonization rates of microorganisms. There appears to be a characteristic relation between bacterial abundance on marine snow and aggregate size (Kiørboe 2000). It is therefore of interest to examine how bacterial colonization rate scales with aggregate size. In both the absence and presence of chemosensory behavior, colonization rate expressed as clearance rate  $\kappa$  is a power function of aggregate size (Fig. 7):

with chemokinetic behavior:

$$\kappa_{+\text{chem}} (\text{cm}^3 \text{s}^{-1}) = 13.65 \times 10^{-3} r_{\text{cm}}^{1.74}, \quad (9a)$$

without chemokinetic behavior:

$$\kappa_{-\text{chem}} (\text{cm}^3 \text{s}^{-1}) = 3.03 \times 10^{-3} r_{\text{cm}}^{1.53}. \quad (9b)$$

In the absence of chemokinetic behavior, encounters between bacteria and a sinking aggregate are almost entirely due to the motility of the bacteria. Chemokinetic behavior has a relatively modest effect on the aggregate colonization rate, both in terms of the scaling (exponents are 1.5 and 1.7) and

in terms of the magnitude. Chemokinesis increases the clearance rate by a factor of 2 for the smallest particles considered ( $r = 0.02$  cm) and by a factor of 5 for the largest particles ( $r = 1.5$  cm). The scaling of colonization rate with aggregate size as suggested here does not translate into a similar scaling of bacterial abundance with aggregate size, because the population dynamics on a particle also include growth and mortality processes. However, the present result may provide a good starting point for modeling—and interpreting observations of—the dynamics of microbial populations on aggregates.

**Impact of aggregate solute plumes on bacterial population growth**—Bacteria that do not colonize the aggregate may utilize the enhanced DOM concentration in the plume. What is the population level effect of the solute plumes trailing behind multiple sinking marine snow aggregates? Do the plumes contribute significantly to the growth of the populations of free bacteria? Does chemokinetic behavior make a significant difference? To examine whether or not there is an impact on the populations of free bacteria, we need be able to integrate the effect for realistic size distributions and concentrations of snow particles.

Individual bacteria take up solutes as they pass through the solute plume. If the uptake rate is limited only by diffusion, the total uptake during passage can be calculated for an individual bacterium and expressed as a fraction of its internal content of the element in question (nitrogen). The diffusion-limited uptake rate for a bacterium is  $4\pi aDC$ , where  $a$  is the radius of the bacterium (assumed to be  $0.5 \mu\text{m}$ ),  $C$  is the modeled amino acid concentration, and  $D$  is again the diffusion coefficient. We summed the total uptake in the plume of all the bacteria that did not collide with the aggregate, and we expressed the result in terms of cell equivalents by dividing by an assumed bacterial nitrogen content of  $10^{-15} \text{mol-N}$ . This value is equivalent to the number of bacteria that could be produced—given a growth yield of 1.0—from the passage of the original number of bacteria through the plume. It can be expressed in terms of a cross-sectional uptake rate in the same way that the bacteria that colonize an aggregate is. The bacterial uptake cross-sectional area multiplied by the aggregate sinking velocity is the bacterial uptake clearance rate (units: fractional uptake  $\text{cm}^3 \text{s}^{-1}$ ),  $\beta$ . It expresses the equivalent volume of water in which all bacteria double their N-content per unit time. We computed this volume-rate for bacteria with and without chemosensory behavior (Fig. 8) and fitted a power relation of the form  $\beta = b_0 r^{b_1}$ , yielding:

$$\beta_{+\text{chemo}} (\text{cm}^3 \text{s}^{-1}) = 0.181 r_{\text{cm}}^{2.67}, \quad (10a)$$

$$\beta_{-\text{chemo}} (\text{cm}^3 \text{s}^{-1}) = 0.072 r_{\text{cm}}^{3.21}. \quad (10b)$$

The effect of chemosensory behavior expressed this way is a substantial factor of 20 enhancement for the smallest aggregates considered ( $r = 0.02$  cm) but is a modest factor of 2 for the largest ( $r = 1.5$  cm) aggregates.

We combined these size-specific clearance rates with aggregate size spectra to assess the total impact of all aggregates in the environment. Particle size spectra are frequently expressed as

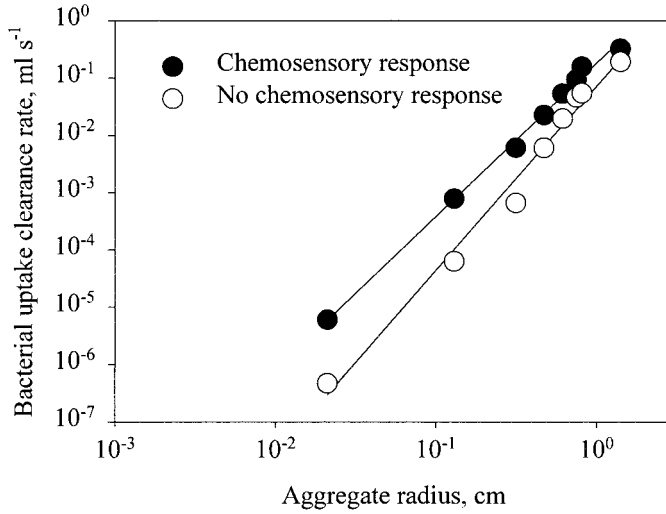


Fig. 8. Bacterial plume utilization, quantified as bacterial uptake clearance rate ( $\beta$ ,  $\text{cm}^3 \text{s}^{-1}$ ), as a function of aggregate radius ( $r$ , cm) and chemosensory behavior. The regression lines are: no chemosensory response,  $\log \beta = -1.14 + 3.21 \log r$ , and with chemosensory response,  $\log \beta = -0.74 + 2.67 \log r$ . Computations are based on bacterial swimming velocity  $v_0 = 100 \mu\text{m s}^{-1}$  and  $\tau_0 = 1$  s. For chemosensory bacteria,  $K_D = 10^{-9} \text{ mol cm}^{-3}$ .

$$n(r) = b_3 r^{-b_4}, \quad (11)$$

where  $n(r)$  is the particle size spectrum (number of particles  $\text{cm}^{-3} \text{cm}^{-1}$ ). The integrated effect of multiple sinking aggregates on bacterial fractional uptake rate ( $\mu$ ) is then given by

$$\mu = \int_{r_1}^{r_2} n(r)\beta(r) dr = \frac{b_3 b_0}{b_1 - b_4 + 1} [r^{b_1 - b_4 + 1}]_{r_1}^{r_2} \quad (\text{if } b_1 - b_4 \neq -1). \quad (12)$$

This property,  $\mu$ , is the average specific uptake rate of suspended bacteria due to the solute plumes trailing behind sinking aggregates. If we assume an N-growth yield of 1, then  $\mu$  is also the average specific growth rate of suspended bacteria. Thus, from knowledge of the coefficients ( $b_0$ ,  $b_1$ ,  $b_3$ , and  $b_4$ ) and the size range of aggregates occurring in a particular environment ( $r_1$ – $r_2$ ), we may assess the potential significance of aggregate-solute-plumes for the growth of free bacteria.

Jackson et al. (1997) and Kiørboe et al. (1998) reported aggregate size spectra and estimates of  $b_3$  and  $b_4$  from Monterey Bay and the Benguela Upwelling Current, respectively. Combining these spectra with the bacterial uptake clearance rates estimated above (Eq. 10) leads to estimates of specific growth rates of free bacteria due to aggregate solute plumes in these areas (Table 2). For bacteria with optimal chemokinetic behavior, estimated growth rates are substantial, on the order of 1.0–10  $\text{d}^{-1}$ . Even in the absence of chemokinetic behavior estimated bacterial growth due to solute plumes is significant, on the order of 0.1–1.0  $\text{d}^{-1}$ .

There are several reports in the literature on number and volume concentrations of marine snow aggregates in surface waters, but, often, proper size spectra have not been reported. In order to utilize that information for a more global

Table 2. Estimated impact of aggregate solute plumes on the specific growth rate of suspended bacteria, estimates of amino acid leakage rate from aggregates, and estimates of equivalent bacterial production. All estimates are made from fits to particle size spectra. The size spectra are characterized by two coefficients,  $b_3$  and  $b_4$ , and have been recorded in the size interval  $r_1$  to  $r_2$ . Data given correspond to geometric mean and range. The data from Monterey Bay consists of spectra recorded once at 10, 15, and 30 m depth by use of multiple instruments. The data from the Benguela consists of spectra recorded twice daily during 6 d. Estimates are made assuming either chemokinetic behavior or no chemokinetic response and have been calculated under the assumption of  $10^{-15} \text{ mol amino acid per bacterium}$ .

Site	$b_3$	$b_4$	Size range $r_1$ – $r_2$ (cm)	Estimated bacterial growth rate, $\text{d}^{-1}$		Amino acid production rate, $\text{mol cm}^{-3} \text{s}^{-1}$	Equivalent bacterial production, $\text{cells cm}^{-3} \text{d}^{-1}$	Source
				+ chemotaxi	– chemotaxi			
Monterey Bay, July	$2.5\text{--}4.1 \times 10^{-5}$	2.96–3.00	$0.5 \times 10^{-4}$ –0.5	0.44 (0.37–0.55)	0.07 (0.06–0.09)	$7.4 \times 10^{-15}$	$6.4 \times 10^5$ ( $5.9\text{--}7.2 \times 10^5$ )	Jackson et al. (1997)
Benguela Current, February	$0.1\text{--}10.4 \times 10^{-3}$	1.6–2.6	0.023–0.50	7.3 (4.0–18.3)	1.4 (0.9–4.0)	$3.6 \times 10^{-15}$ ( $2.2\text{--}5.5 \times 10^{-15}$ )	$2.1 \times 10^5$ ( $0.1\text{--}4.8 \times 10^5$ )	Kiørboe et al. (1998)

assessment, we note that the volume fraction of suspended particles,  $VF$ , is given by

$$VF = \int_{r_1}^{r_2} \frac{4}{3} \pi r^3 n(r) dr = \int_{r_1}^{r_2} \frac{4}{3} \pi b_3 r^{3-b_4} dr$$

$$= \frac{4}{3} \pi b_3 \frac{1}{4-b_4} [r^{4-b_4}]_{r_1}^{r_2}. \quad (13)$$

If we know the volume fraction of suspended particles, which is often reported, and assume an exponent of the size spectrum,  $b_4 = 3$  (cf. Jackson et al. 1997), then we can estimate  $b_3$  from the above equation. Alldredge and Silver (1988) compiled information on volume concentrations of marine snow aggregates in surface waters. Such concentrations are highly variable, 10–7,000 ppm, with a geometric mean of  $\sim 300$  ppm. If we assume that marine snow in the reported studies considers particles in the 0.05–1 cm (radius) size range, then the geometric mean volume concentration of aggregates would contribute an estimated specific growth rate of bacteria (with chemokinetic behavior) of  $1.9 \text{ d}^{-1}$ . At the high extreme (7,000 ppm), the potential effect would be substantial ( $45 \text{ d}^{-1}$ ), at the lower end, the effect would be small ( $0.06 \text{ d}^{-1}$ ). For bacteria without chemokinetic behavior, the estimated rates are 0.01, 0.33, and  $7.59 \text{ d}^{-1}$ , for the low-est, median, and highest snow concentrations reported.

These numbers should be compared with direct estimates of “bulk” bacterial growth rates. Mean growth rates of bacteria in the upper ocean are reported in the range  $0.05\text{--}1.0 \text{ d}^{-1}$  for habitats ranging from the tropics to the arctic (Ducklow 2000). This would suggest that solute plumes from sinking aggregates may provide very significant growth habitats for suspended bacteria.

The above estimates are very crude for a number of reasons. In particular, (1) aggregates may sink slower than anticipated here, (2) bacteria are not perfect absorbers, (3) the background concentration is different from zero, (4) bacterial uptake in the plume will lower concentrations and resulting uptake rates, (5) turbulence may dissipate the solute plume, and (6) the use of spectral slopes to calculate particle distributions does not capture all the complexities of size distributions.

The relation between sinking velocity and aggregate size assumed here is that from Alldredge and Gotschalk (1988) and appears to provide upper estimates of aggregate sinking velocities. Other authors have reported size-specific sinking velocities that are an order of magnitude less (e.g., Asper 1987; Pilskaln et al. 1998). If the aggregates sink slower than anticipated here, then our conclusion is conservative, because advection diminishes the extension of the solute plume. Computations made for particles in the considered size range and on the assumption that sinking velocity is an order of magnitude less than predicted by Eq. 1 lead to estimates of  $\beta$  that are more than an order of magnitude higher than those in Fig. 8. For the smallest particles considered, the bacteria are in fact able to follow the sinking aggregate and, hence, never leave the plume.

Nutrient uptake in bacteria seems not to be limited only by the diffusive transport rate but may be reaction limited to some extent as well. Estimates of maximum amino acid

uptake rates ( $V_{\max}$ ) reported for field populations of bacteria (e.g., Carlucci et al. 1986; Fuhrman and Ferguson 1986; Suttle et al. 1991) appear to be substantially less than diffusion would be able to account for. This difference is likely to be much less under nutrient limitation but may still prevail. Thus, Koch (1997) found that nutrient uptake in *E. coli* bacteria is factor of at least 5 less than that predicted from diffusion calculations, possibly because of impediment of uptake through the outer membrane, which is found in gram-negative bacteria. Overall, this may lead to a somewhat inflated expectation to the effect of aggregate-generated solute plumes.

We have assumed a background concentration of zero. The plume concentrations computed here are concentrations in excess of background. Therefore, the estimated uptake rates of bacteria inside the plume are “excess” uptake rates—estimates of what extra the bacteria gain. However, a background concentration different from zero will lead to lower concentration gradients around the sinking aggregates and therefore to a reduced effect of a chemokinetic response. The true value of the plume is therefore somewhere between that estimated for bacteria with and without a chemokinetic response.

These calculations have ignored any decrease in nutrient concentration in the plume associated with bacterial uptake. The larger a fraction of nutrient uptake that occurs in the plume, the greater the change in plume concentration. Because we have assumed that nutrient uptake is diffusion limited, a decrease in plume concentration would decrease bacterial uptake rates. The more important that bacterial uptake in the plume is, the more important it is to address this issue.

Turbulence may dissipate solute patches. The lengths of the plumes considered in this study are on the order of 100 particle radii. Thus, for the largest aggregates, the computed plumes are on the order of 1 m, and the timescale at which they exist (plume length/aggregate sinking velocity) is 10–15 min. Obviously, turbulence will affect such long patches in the course of such long times. Plumes will meander, stretch, and break up because of turbulence. These processes do not per se change plume concentrations. Stretching, however, will make the plume narrower and, therefore, increase the significance of molecular diffusion in dissipating the plume. A numerical simulation is required to examine the effect of turbulence on plume extension and persistence and the consequences for bacteria.

Finally, there are limitations on the use of size spectra. The size ranges considered reflect the limitations of the instruments used to record the spectra rather than the true size range of particles in the environment. Thus, the effects of solute plumes may be underestimated if particles larger or smaller than those recorded are abundant. Also, differences in concentration that are 2 or more times that predicted by the spectrum are small, compared with the large size range used to compute the spectrum, but can represent significant reservoirs of mass.

*Stoichiometric considerations*—Bacterial growth due to solutes leaking out of aggregates is, of course, limited by the total amount of solutes provided this way. Stoichiometric

considerations therefore provide an upper limit of plume-generated bacterial growth.

The total amino acid leakage from all aggregates combined ( $\text{mol cm}^{-3} \text{ s}^{-1}$ ) is

$$\int_{r_1}^{r_2} n(r)Q(r) dr = \frac{10^{-12} \cdot b_3}{1.5 - b_4 + 1} [r^{1.5-b_4+1}]_{r_1}^{r_2} \quad (14)$$

Estimates of amino acid production this way for the data of Jackson et al. (1997) and Kjørboe et al. (1998) are similar and are on the order of  $5 \times 10^{-15} \text{ mol amino acid cm}^{-3} \text{ s}^{-1}$  (Table 2). If one bacterium contains  $10^{-15} \text{ mol amino acid}$  (or N), then this corresponds to a bacterial production of  $5 \times 10^5 \text{ bacteria cm}^{-3} \text{ d}^{-1}$ . A more global assessment based on the data compiled by Alldredge and Silver (1988) and with the same assumptions as above leads to bacterial production rates of  $0.03 \times 10^5$ ,  $10^5$ , and  $20 \times 10^5 \text{ cells cm}^{-3} \text{ d}^{-1}$  (minimum, geometric mean, and maximum, respectively). These estimates are close to typical bacterial production rates reported from surface waters,  $0.05\text{--}2.75 \times 10^5 \text{ cells cm}^3 \text{ d}^{-1}$  (computed from the data-compilation in table 5 of Ducklow 2000 by assuming  $20 \times 10^{-15} \text{ g C cell}^{-1}$ ).

## Conclusions

Overall, these considerations suggest that aggregates may be important sources of DOM for bacterial growth in the upper ocean and that the solute plumes in the wake of sinking aggregates can be important growth habitats for suspended bacteria. The DOM stemming from aggregates relies on solubilization processes in the aggregates themselves, and the quantitative importance of these processes for DOM production depends on the size distribution and abundance of aggregates. Both are relatively poorly understood or known.

There are relatively few reliable observations of particle or aggregate size spectra available in the literature; most of the available ones consider only a relatively narrow size range. Reliable size spectra are difficult to obtain, in part because different instruments measure particle size differently. Furthermore, the ecologically important particle properties include more than just diameter but also settling velocity and composition. Knowing several properties would allow the calculation of more informative spectra, such as a dimensional spectrum that describes the distribution of particles as functions of diameter and mass (e.g., Jackson 1998).

The dissolution of particles in aggregates is due to bacteria that are exuding ectoenzymes (Smith et al. 1992). Ecto-enzyme activity can be high in aggregates because of the combined effect of ectoenzyme production from all residing bacteria, and solubilization of particulate material is therefore potentially enhanced in aggregated relative to solitary particles. The bacteria (or their ancestors) residing on an aggregate originally colonized from the ambient water. Ecto-enzyme production is probably a relatively expensive process, and one could therefore envisage that ectoenzyme production is regulated. Many bacteria leak signal molecules at very low rates, and these signal molecules regulate the expression of certain genes (Eberl 1999). Such "quorum sensing" offers a potential mechanism by which ectoenzyme production could be regulated. A combination of high mo-

tility in colonizing bacteria, a chemokinetic response to chemical gradients, and regulation of ectoenzyme production by signal molecules makes the transformation of particulate organic matter to DOM in aggregates a potentially very efficient process. These processes not only may account for the high bacterial activity typical of aggregates but may also have wider implications for microbial processes in the water column.

## References

- ALLDREDGE, A.L. 2000. Interstitial dissolved organic carbon (DOC) concentrations within sinking marine aggregates and their potential contribution to carbon flux. *Limnol. Oceanogr.* **45**: 1245–1253.
- , AND C. GOTSCHALK. 1988. In situ settling behaviour of marine snow. *Limnol. Oceanogr.* **33**: 339–351.
- , AND M. W. SILVER. 1988. Characteristics, dynamics and significance of marine snow. *Prog. Oceanogr.* **20**: 42–82.
- ASPER, L. L. 1987. Measuring the flux and sinking speed of marine snow aggregates. *Deep-Sea Res.* **34**: 1–17.
- BARBARA, G. M., AND J. G. MITCHELL. 1996. Formation of 30- to 40-micrometer-thick laminations by high-speed marine bacteria in microbial mats. *Appl. Environ. Microbiol.* **62**: 3985–3990.
- BOWEN, J. D., K. D. STOLZENBACH, AND S. W. CHRISHOLM. 1993. Simulating bacterial clustering around phytoplankton cells in a turbulent ocean. *Limnol. Oceanogr.* **38**: 36–51.
- BLACKBURN, N., T. FENCHEL, AND J. MITCHELL. 1998. Microscale nutrient patches in planktonic habitats shown by chemotactic bacteria. *Science* **282**: 2254–2256.
- BROWN, D. A., AND H. C. BERG. 1974. Temporal simulation of chemotaxis in *Escherichia coli*. *Proc. Natl. Acad. Sci.* **71**: 1388–1392.
- CARLUCCI, A. F., D. B. CRAVEN, K. J. ROBERTSON, AND S. M. HEINRICH. 1986. Microheterotrophic utilization of dissolved free amino acids in depth profiles of Southern California Borderland basin waters. *Oceanol. Acta* **9**: 89–96.
- DUCKLOW, H. 2000. Bacterial production and biomass in the oceans, p. 85–120. *In* D. L. Kirchman [ed.], *Microbial ecology of the oceans*. Wiley-Liss.
- DUSENBERY, D. B. 1998. Fitness landscapes for effects of shape on chemotaxis and other behaviors of bacteria. *J. Bacteriol.* **180**: 5978–5983.
- EBERL, L. 1999. N-Acyl Homoserinelactone-mediated gene regulation is gram-negative bacteria. *Syst. Appl. Microbiol.* **22**: 493–506.
- FENCHEL, T. 1994. Motility and chemosensory behaviour of the sulphur bacterium *Thiovulum majus*. *Microbiology* **140**: 3109–3116.
- FUHRMAN, J. A., AND R. L. FERGUSON, R.L. 1986. Nanomolar concentrations and rapid turnover of dissolved free amino acids in seawater: Agreement between chemical and microbiological measurements. *Mar. Ecol. Prog. Ser.* **33**: 237–242.
- GROSSART, H.-P., AND M. SIMON. 1998. Bacterial colonization and microbial decomposition of limnetic organic aggregates (lake snow). *Aquat. Microb. Ecol.* **15**: 127–140.
- JACKSON, G. A. 1987. Simulating chemosensory response of marine microorganisms. *Limnol. Oceanogr.* **32**: 1253–1266.
- . 1989. Simulation of bacterial attraction and adhesion to falling particles in an aquatic environment. *Limnol. Oceanogr.* **34**: 514–530.
- . 1998. Using fractal scaling and two dimensional particle size spectra to calculate coagulation rates for heterogeneous systems. *J. Colloid Interface Sci.* **202**: 20–29.
- , AND J. J. MORGAN. 1978. Trace metal-chelator interactions

- and phytoplankton growth in seawater media: Theoretical analysis and comparison with reported observations. *Limnol. Oceanogr.* **23**: 268–282.
- , R. MAFFIONE, D. K. COSTELLO, A. L. ALLDREDGE, B. E. LOGAN, AND H. G. DAM. 1997. Particle size spectra between 1  $\mu\text{m}$  and 1 cm at Monterey Bay determined using multiple instruments. *Deep-Sea Res.* **44**: 1739–1767.
- KJØRBOE, T. 2000. Colonization of marine snow aggregates by invertebrate zooplankton: Abundance, scaling, and possible role. *Limnol. Oceanogr.* **45**: 479–484.
- , H. PLOUG, AND U.H. THYGESSEN. 2001. Fluid motion and solute distribution around sinking aggregates. I. Small scale fluxes and heterogeneity of nutrients in the pelagic environment. *Mar. Ecol. Prog. Ser.* **211**: 1–13.
- , P. TISELIUS, B. MITCHELL-INNES, J. L. S. HANSEN, A. W. VISSER, AND X. MARI. 1998. Intensive aggregate formation with low vertical flux during an upwelling-induced diatom bloom. *Limnol. Oceanogr.* **43**: 104–116.
- , AND A. W. VISSER. 1999. Predator and prey perception in copepods due to hydromechanical signals. *Mar. Ecol. Prog. Ser.* **179**: 81–95.
- KOCH, A. L. 1997. Microbial physiology and ecology of slow growth. *Microbiol. Molec. Biol. Rev.* **61**: 305–318.
- LAMPERT, W. 1978. Release of dissolved organic carbon by grazing zooplankton. *Limnol. Oceanogr.* **23**: 831–834.
- LUCHSINGER, R. H., B. BERGERSEN, AND J. G. MITCHELL. 1999. Bacterial swimming strategies and turbulence. *Biophys. J.* **77**: 2377–2386.
- MESIBOV, R., G. W. ORDAL, AND J. ADLER. 1973. The range of attractant concentrations for bacterial chemotaxis and the threshold and size of response over this range. *J. Gen. Phys.* **62**: 203–223.
- MITCHELL, J. G., AND G. M. BARBARA. 1999. High speed marine bacteria use sodium-ion and proton driven motors. *Aquat. Microbial. Ecol.* **18**: 227–233.
- , L. PEARSON, A. BONAZINGA, S. DILLON, H. KHOURI, AND R. PAXINOS. 1995a. Long lag times and high velocities in the motility of natural assemblages of marine bacteria. *Appl. Env. Microbiol.* **61**: 877–882.
- , L. PEARSON, AND S. DILLON, S. 1996. Clustering of marine bacteria in seawater enrichments. *Appl. Env. Microbiol.* **62**: 3716–3721.
- , L. PEARSON, S. DILLON, AND K. KANTALIS. 1995b. Natural assemblages of marine bacteria exhibit high-speed motility and large accelerations. *Appl. Env. Microbiol.* **61**: 4436–4440.
- PILSKALN, C. H., C. LEHMAN, J. F. PADUAN, AND M. W. SILVER. 1998. Spatial and temporal dynamics in marine aggregate abundance, sinking rate and flux: Monterey Bay, central California. *Deep-Sea Res. II.* **45**: 1803–1837.
- SMITH, D. C., M. W. SILVER, A. L. ALLDREDGE, AND F. AZAM. 1992. Intense hydrolytic activity on marine aggregates and implications for rapid particle dissolution. *Nature* **359**: 139–141.
- SUTTLE, C. A., A. M. CHAN, AND J. A. FUHRMAN. 1991. Dissolved free amino acids in the Sargasso Sea: Uptake and respiration rates, turnover times, and concentrations. *Mar. Ecol. Prog. Ser.* **70**: 189–199.
- URBAN-RICH, J. 1999. Release of dissolved organic carbon from copepod fecal pellets in the Greenland Sea. *J. Exp. Mar. Biol. Ecol.* **34**: 107–124.
- VETTER, Y. A., J. W. DEMING, P. A. JUMARS, AND B. B. KRIEGER-BROCKETT. 1998. A predictive model of bacterial foraging by means of freely released extracellular enzymes. *Microb. Ecol.* **36**: 75–92.
- VISSER, A. W., AND P. R. JONSSON. 2000. On the reorientation of non-spherical particles in a feeding current. *J. Plankton Res.* **22**: 761–777.

Received: 12 January 2001

Accepted: 19 April 2001

Amended: 9 May 2001